Available online at www.sciencedirect.com
ScienceDirect
Journal of the European Ceramic Society 27 (2007) 2273–2280
www.elsevier.com/locate/jeurceramsoc

Structure and microwave dielectric property relations in $(Ba_{1-x}Sr_x)_5Nb_4O_{15}$ system

Chun-Te Lee [a,*], Chien-Chih Ou [a], Yi-Chang Lin [a], Chi-Yuen Huang [a], Che-Yi Su [b]

[a] *Department of Resources Engineering, National Cheng Kung University, No. 1, Ta-Hsueh Road, Tainan 701, Taiwan, ROC*
[b] *R&D Technology Center, Yageo Co. Ltd., 16 West 3rd Street, NEPZ Kaohsiung 811, Taiwan, ROC*

Received 18 June 2006; accepted 28 July 2006
Available online 18 September 2006

Abstract

The effects of strontium substitution for barium on the structure and microwave dielectric properties of $Ba_5Nb_4O_{15}$ compounds is investigated using X-ray diffraction, Raman spectroscopy, and microwave dielectric properties measurement. The symmetric stretching vibration of Ba-rich compounds splits into two narrow Raman-active modes and indicates the existence of a strong anharmonic lattice. Nevertheless, the symmetry changes from $P\bar{3}m1$ to $P\bar{3}c1$ for the Sr-rich compounds. The relative permittivity (ε_r) and temperature coefficient of resonant frequency (τ_f) increases linearly with an increase of strontium content in Ba-rich compounds, but decreases in Sr-rich compounds. The transition of symmetry influences the variation of ε_r and τ_f. The behavior of ε_r and τ_f can also be correlated to the variation of symmetric stretching vibrations of NbO_6 octahedra and (c/a) ratio of lattice parameter in the unit cell.

Keyword: $(Ba_{1-x}Sr_x)_5Nb_4O_{15}$; X-ray methods; Spectroscopy; Dielectrics properties

1. Introduction

The $A_5B_4O_{15}$ (A = Ba, Sr, Mg, Ca; B = Nb, Ta) dielectric ceramics have good microwave dielectric properties, including high relative permittivity (ε_r), high quality factor (Q), and low temperature coefficient of resonator frequency (τ_f). The ceramics show ε_r in the range of 11–51, $Q \times f = 2400$–$88{,}000$ GHz and τ_f in the range -73 to $+232$ ppm/°C.[1–3] This type of materials is called cation-deficient perovskites if written in the perovskite form (ABO_3), and $A_5B_4O_{15}$ is reduced to $AB_{0.8}O_3$. There is a vacancy of 0.2B cation per 1A cation, i.e., overall 1B cation vacancy per 5A cations. Galasso et al.[4] showed that these compounds have hexagonal structure and crystallized them in the $P\bar{3}m1$ space group. They also have the closest packing of oxygen and barium ions into five layers. The tantalum or niobium ions are located in the octahedral holes between layers. One layer of the octahedral hole does not have tantalum or niobium ions to obtain the charge neutrality. Therefore, there is an empty octahedra, which results in the loss of face sharing on the NbO_6 sublattice, and this structure implies strong anharmonicity.

Jawahar et al.[1] showed that a considerable distortion can be noted in the empty octahedra which has the great electrostatic valence imbalance. The $Ba_5Nb_4O_{15}$ shows a hexagonal structure where $\varepsilon_r = 39$, $Q \times f = 23{,}700$ and $\tau_f = 78$ ppm/°C. The $Ba_5Ta_4O_{15}$ has a lower $\varepsilon_r = 28$ than that of $Ba_5Nb_4O_{15}$, even though its tantalum has larger ionic polarizability. This is because the lattice of $Ba_5Ta_4O_{15}$ is stable whereas that of $Ba_5Nb_4O_{15}$ could collapse to a lower symmetry. Lattice anharmonicity causes a relatively higher permittivity for $Ba_5Nb_4O_{15}$ compound.

Massa et al.[5] showed that $Ba_5Nb_4O_{15}$ compound is characterized by such a strong anharmonic lattice where the symmetric stretching vibration of the empty octahedra splits into two narrow Raman-active modes. This indicates that the lattice of $Ba_5Nb_4O_{15}$ has a small local departure from the reported centrosymmetric $D^3_{3d} - P\bar{3}m1$ space group and it is close to collapsing into a lower symmetry structure. Shannon et al.[6] showed that the octahedral environment of the tantalum atoms become distorted because of the required local charge balance in $Ba_5Ta_4O_{15}$ compound. The shortest and longest Ta–O distance in the octahedra are 1.86 ± 0.02 Å and 2.22 ± 0.03 Å,

* Corresponding author. Tel.: +886 7 3614101; fax: +886 7 9627991.
E-mail address: ct.chunte@gmail.com (C.-T. Lee).

0955-2219/$ – see front matter © 2006 Elsevier Ltd. All rights reserved.
doi:10.1016/j.jeurceramsoc.2006.07.022

respectively. Pagola et al.[7] showed that the polyhedra at both metal positions can be described as very distorted octahedra and their bond distances range from 1.93 to 2.22 Å in $Mg_5Nb_4O_{15}$ and $Mg_5Ta_4O_{15}$ compounds. Moreover, the distortion and anharmonic lattice were found in the cation-deficient perovskites from previous investigation. Meanwhile, the effect of structure transition on microwave dielectric properties has not been clarified in previous investigation.

Kim et al.[8–11] proposed that the addition of B_2O_3 to $Ba_5Nb_4O_{15}$ results in lowering the sintering temperature from 1400 to 925 °C. This is due to the formation of liquid phase such as BaB_2O_4. Furthermore, the τ_f of low-fired $Ba_5Nb_4O_{15}$ is modified to 0 ppm/°C by the formation of second phase $BaNb_2O_6$ because it has a large and negative τ_f, −800 ppm/°C. This means that the $Ba_5Nb_4O_{15}$ compound has excellent dielectric properties that make it suitable for microwave communication system and low-temperature co-fired ceramic (LTCC).

Compounds with $(Ba_{1-x}Sr_x)_5Nb_4O_{15}$ composition have been reported to show high permittivity and low loss in microwave frequency region[12]. The ε_r and τ_f seem to show a remarkable relation with the Sr^{2+} substitution in $(Ba_{1-x}Sr_x)_5Nb_4O_{15}$ system. Ratheesh et al.[13] proposed that the relative permittivity of $(Ba_{5-x}Sr_x)Nb_4O_{15}$ system can be correlated to the variation of symmetric stretching vibration of NbO_6 octahedra from Raman analysis. Several authors[14–16] have used the analysis of vibration spectra to study the lattice distortion of microwave dielectric ceramics, and investigate the origin of relative permittivity.

In this investigation, the $(Ba_{1-x}Sr_x)_5Nb_4O_{15}$ ceramic was prepared and the crystal structure was refined by Rietveld method to clarify the relation between structure and microwave dielectric properties with XRD patterns and Raman spectra.

2. Experimental procedure

Samples of $(Ba_{1-x}Sr_x)_5Nb_4O_{15}$ system with $x = 0$, 0.1, 0.2, 0.4, 0.6, 0.8 and 1 were prepared using conventional solid-state reaction. $BaCO_3$, $SrCO_3$ and Nb_2O_5 (which have 99.5% purity) were mixed with ball milling method by ethanol and yttrium-stabilized zirconia ball for 3 h. The slurry was dried and calcined at 1250 °C for 12 h in air. The calcined powder was milled again for 6 h, dried, sieved and compacted in cylinders and sintered at 1450 °C for 4 h. The phase composition was investigated by X-ray diffraction (Siemens D5000) using graphite-filtered Cu K_1 ($\lambda = 1.5406$ Å) radiation between $2\theta = 10°$ and 100°, a step size of 0.02° 2θ/s and a sampling time of 8 s/step. The XRD diffraction patterns were analyzed by the Rietveld method using the GSAS program.[17] A pseudo-Voigt function was used to generate the line-shape of the diffraction peaks. The microstructures of the polished samples were investigated and analyzed using SEM (HitachiS4100). Raman spectra were measured by Dilor XY Raman spectrometer, detecting time of 10 s, and resolution of 1 cm^{-1}. Samples were excited by Ar ion laser beam with a wavelength of 515 nm and power output of 100 mW.

The relative permittivity (ε_r) and quality factor (Q) at microwave frequency were measured with the Hakki-Coleman dielectric resonator method, using a HP8757D network analyzer and a HP8350B sweep oscillator. The Q values were measured using a TE_{011} resonant peak, and τ_f was obtained by measuring the resonant frequency in the temperature range of 25–85 °C. The τ_f value (ppm/°C) was calculated by noting the change in resonant frequency.

3. Results

Fig. 1 shows the X-ray diffraction pattern of the $(Ba_{1-x}Sr_x)_5Nb_4O_{15}$ system that shows the single phase and isostructural nature of the said compounds. The patterns were indexed based on hexagonal symmetry for $Ba_5Nb_4O_{15}$ compound. The Sr^{2+} ion can fully substitute into the Ba-site without the occurrence of the second phase.

Fig. 2 shows the typical microstructures of $(Ba_{1-x}Sr_x)_5Nb_4O_{15}$ ceramics, which have elongated grains. The abnormal grain growth and elongated grain caused the sintered density to reach only below 96%. The relative density reached above 93% while sintering at 1450 °C/4 h. The grain size seemed to decrease with Sr^{2+} substitution and showed a bi-model distribution in the microstructure.

In order to clarify the effect of strontium substitution for barium ion in the structure, the lattice parameter and symmetry were determined by Rietveld analysis. Weiden et al.[18] found that the $Sr_5Nb_4O_{15}$ compound develops a monoclinic distortion which leads to a unit cell with symmetry P2/m with twice the volume of the hexagonal cell. Ratheesh et al.[13] concluded that $Sr_5Nb_4O_{15}$ has a hexagonal structure in accordance with the report of Whiston.[19] However, the structure determination of $Sr_5Nb_4O_{15}$ started with the presumption that it would crystallize in a similar structure with $Ba_5Nb_4O_{15}$ hexagonal compound with $P\bar{3}m1$ pace group. The refinements were successfully performed by the symmetry of space group $P\bar{3}m1$ and $P\bar{3}c1$ for Ba-rich and Sr-rich compounds, respectively. The symmetry of $Sr_5Nb_4O_{15}$ showed a $P\bar{3}c1$ space group with better reliability factors and goodness of fit indicator as shown in Table 1. The refinement of $Sr_5Nb_4O_{15}$ was consistent with the report of

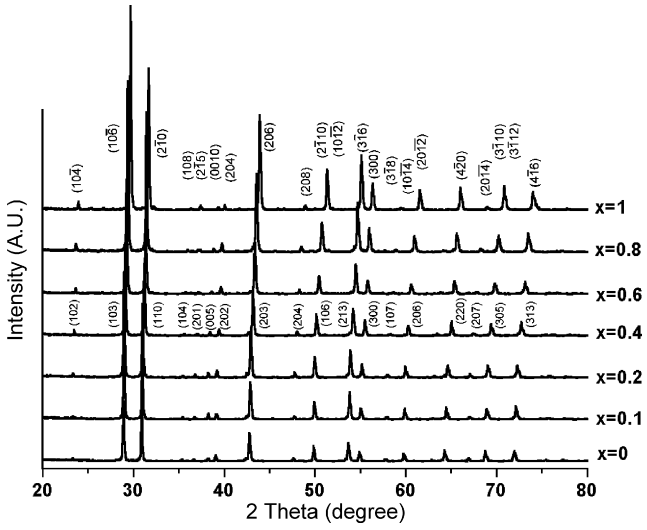

Fig. 1. X-ray diffraction patterns of the $(Ba_{1-x}Sr_x)_5Nb_4O_{15}$ compounds.

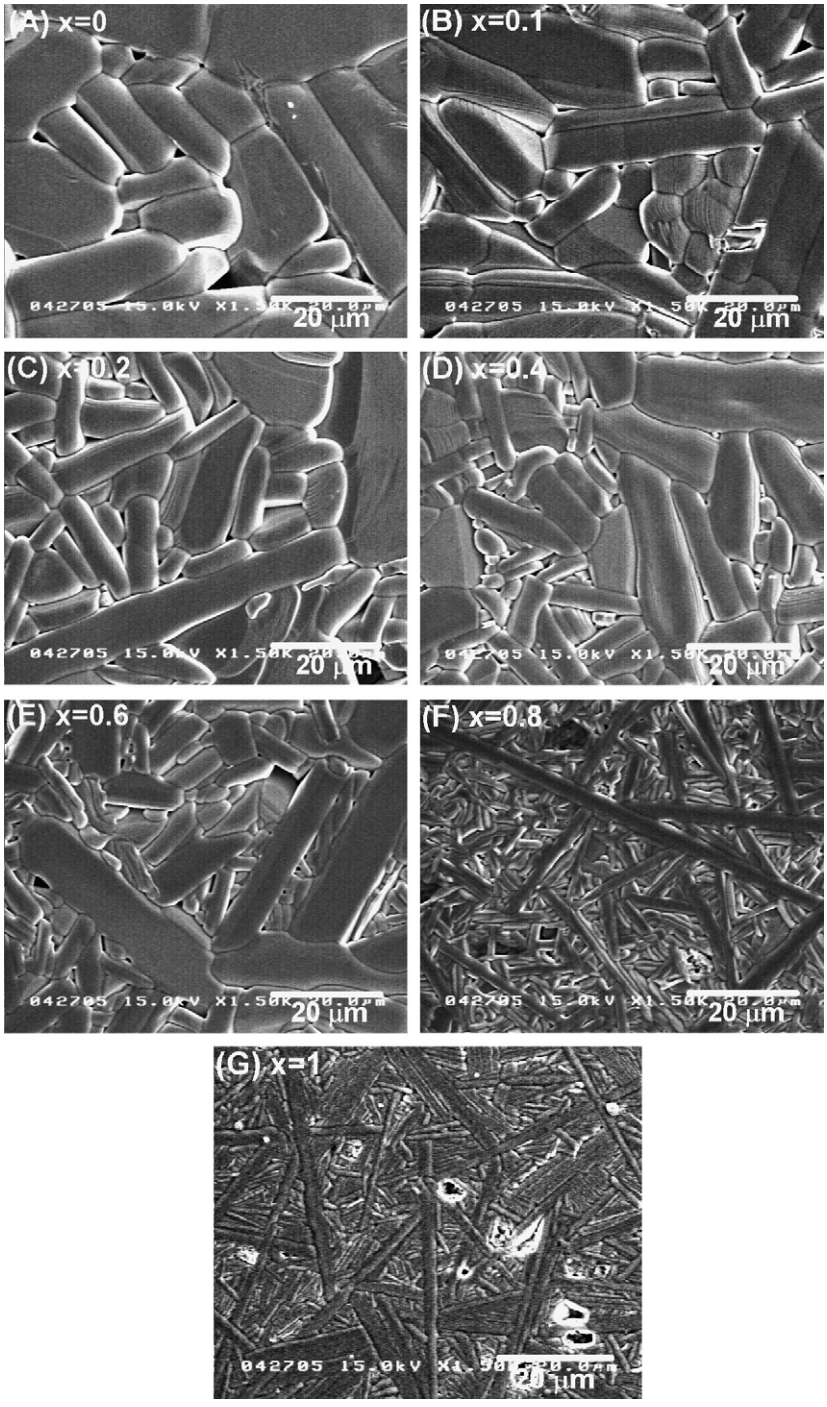

Fig. 2. Microstructure of the $(Ba_{1-x}Sr_x)_5Nb_4O_{15}$ compounds.

Teneze et al.[20] and it was confirm to have hexagonal symmetry. The c-parameter is doubled due to an anti-tilting of octahedra (∼15°) around the *c*-axis. Fig. 3 shows the excellent agreement between the observed and calculated profile of the XRD patterns for $Ba_5Nb_4O_{15}$ and $Sr_5Nb_4O_{15}$ compound. The refined lattice parameters, unit cell volumes, reliability factors, and goodness of fit indicator are listed in Table 1. The symmetry of crystal structure was changed from $P\bar{3}m1$ to $P\bar{3}c1$ while strontium substitution increased to Sr-rich compounds. Therefore, the X-ray diffraction patterns in Fig. 1 were indexed with $P\bar{3}m1$ and $P\bar{3}c1$ symmetry for Ba-rich and Sr-rich compounds, respectively.

Fig. 4 shows the crystal structure of $Ba_5Nb_4O_{15}$ compound with refined data. The structure consisted of five BaO_3 close-packed layers and niobium ions located in corner-sharing octahedral holes between layers. No niobium ion was observed between the third and the fourth layer. The bond angle of O(3)–Nb(2)–O(3) showed great departure from the angle of 90° expected for an ideal octahedra. The bond lengths of niobium-oxygen showed great variation for O(3) than for the O(2) and

Table 1
The refined lattice parameters, unit cell volumes, reliability factors and goodness of fit indicator for $(Ba_{1-x}Sr_x)_5Nb_4O_{15}$ compounds

Composition (x)	Space group	Lattice parameters		Unit cell volume (Å^3)	R_{wp}	R_p	χ^2
		a (Å)	c (Å)				
0.0	$P\bar{3}m1$	5.7948 (0)	11.7887 (1)	342.8210	11.99	7.58	1.8210
0.1	$P\bar{3}m1$	5.7798 (0)	11.7741 (1)	340.6350	10.79	7.08	1.4580
0.2	$P\bar{3}m1$	5.7639 (0)	11.7558 (1)	338.3310	10.30	6.93	1.3360
0.4	$P\bar{3}m1$	5.7351 (0)	11.7193 (1)	333.8190	10.28	6.72	1.3550
0.6	$P\bar{3}m1$	5.7095 (0)	11.6642 (1)	329.2960	12.09	7.44	1.9150
	$P\bar{3}c1$	5.7123 (0)	11.3393 (1)	659.5460	10.26	8.30	1.5266
0.8	$P\bar{3}m1$	5.6833 (0)	11.5757 (1)	323.8030	11.33	6.87	1.6960
	$P\bar{3}c1$	5.6855 (0)	11.1589 (1)	648.3130	7.85	7.15	1.2071
1.0	$P\bar{3}m1$	5.6567 (0)	11.4599 (1)	317.5720	13.64	8.23	2.2310
	$P\bar{3}c1$	5.6852 (0)	11.9158 (1)	641.4410	7.72	7.15	1.1674

R_{wp}: the reliability factor of weighted patterns; R_p: the reliability factor of patterns; χ^2: goodness of fit indicator = $(R_{wp}/R_{exp.})^2$.

O(1) oxygen ions. A considerable distortion was noted with the O(3) position, which may be due to the great electrostatic valency imbalance at this position. The Nb(2) octahedra were noted to have large differences of 1.871 and 2.266 Å for the bond length of Nb(2)–O(3) and Nb(2)–O(2), respectively. Fig. 5 shows the crystal structure of $Sr_5Nb_4O_{15}$ compound with $P\bar{3}c1$ symmetry. The c-parameter was doubled with two formula units per cell ($Z=2$). The bond lengths and angles of NbO_6 octahedra in $Sr_5Nb_4O_{15}$ showed great departure from that of ideal octahedra and indicated larger distortion than $Ba_5Nb_4O_{15}$ compound.

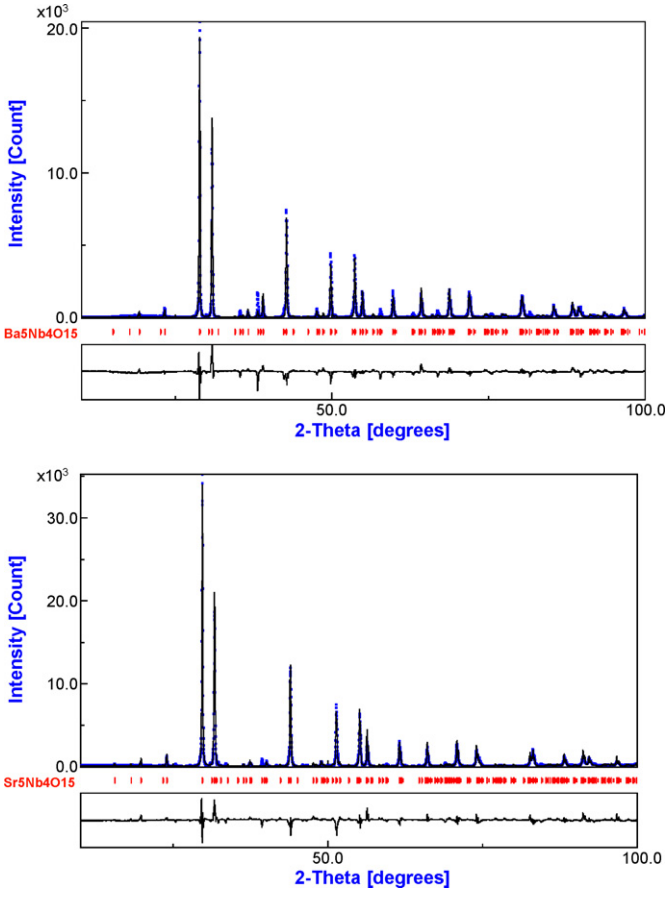

Fig. 3. Observed (cross), calculated (solid lines), and difference (bottom) X-ray diffraction patterns for $Ba_5Nb_4O_{15}$ and $Sr_5Nb_4O_{15}$compound.

The lattice parameter, c and a, decreased linearly with the increase of Sr^{2+} substitution because the ionic radius of Sr^{2+} (1.54 Å) was smaller than Ba^{2+} (1.74 Å). Fig. 6 shows the lattice parameter as a function of strontium substitution. This indicates that the cell volume and lattice parameter, c and a, decreased linearly with the increase of strontium content in Ba-rich compounds. Nevertheless, a linear increase of (c/a) ratio with strontium substitution showed that the unit cell has a stretch along the c-axis in Ba-rich compounds. However, the lattice parameter (c, a and c/a ratio) and cell volume decreased with the increase of strontium content in Sr-rich compounds with $P\bar{3}c1$ symmetry.

The microwave dielectric properties of $(Ba_{1-x}Sr_x)_5Nb_4O_{15}$ ceramics are described in Fig. 7. It was evident that the ε_r and τ_f increased with an increase of strontium content to $x=0.4$ ($Ba_3Sr_2Nb_4O_{15}$), and then decreased later on. Similarly, a distinct correlation was noted between symmetry transition of crystal structure and microwave dielectric properties (ε_r and τ_f). Nevertheless, the substitution of Sr^{2+} ions at the Ba-sites drastically reduced the quality factor. Higher loss of grain boundaries with smaller grain size could be one of the reasons for the degradation of quality factor. However, the grain size did not cause any obvious influence on the ε_r and τ_f.

The spectra of $(Ba_{1-x}Sr_x)_5Nb_4O_{15}$ compounds were very similar to those of pure compounds with $x=0$ and 1, as shown in Fig. 8. The structure of $Sr_5Nb_4O_{15}$ should be similar to $Ba_5Nb_4O_{15}$ with hexagonal symmetry. Two groups of strong Raman active modes were observed at 800 and 310 cm^{-1}. They were assigned to the symmetric stretching modes and bending modes of NbO_6 octahedra with O_h symmetry, respectively. However, the departure from O_h symmetry resulted in the line broadening or splitting of Raman spectrum.

The strongest band at 800 cm^{-1} could be associated with short niobium–oxygen bond distances. The large splitting was observed for the symmetric stretching region of A_{1g} mode for Ba-rich compounds. In the Raman spectrum of $Ba_5Nb_4O_{15}$

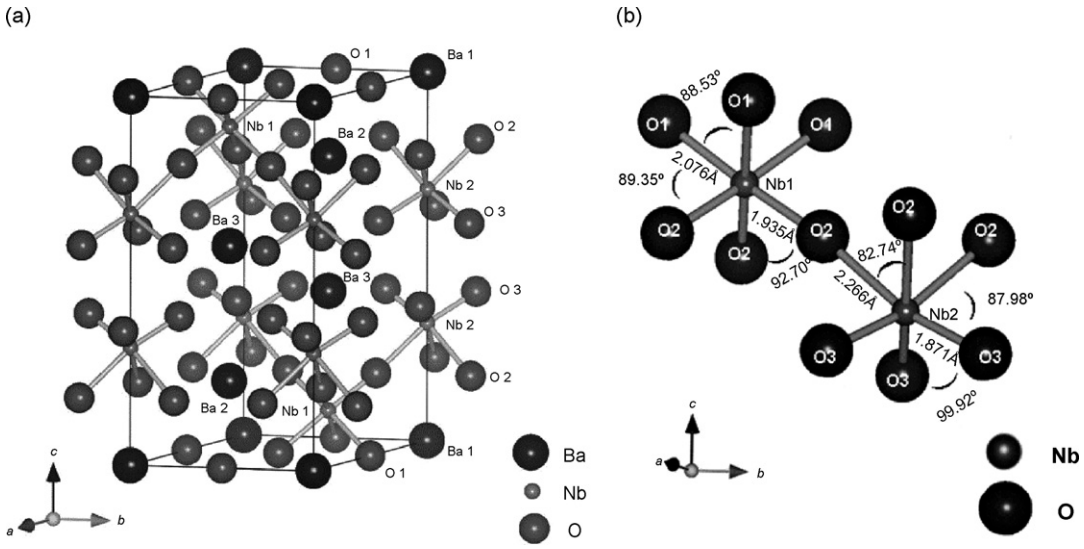

Fig. 4. (a) Crystal structure of $Ba_5Nb_4O_{15}$ compound with refined XRD data. (b) Description of bond lengths and angles in NbO_6 octahedra for $Ba_5Nb_4O_{15}$ compound.

($x = 0$), symmetric stretching mode of NbO_6 octahedra was split into two modes at 773 and 846 cm^{-1}. This doublet was shifted toward higher wave-number region with the increase of strontium substitution at $x \leq 0.4$. This indicates that the distortion of NbO_6 octahedra exists stably in the Ba-rich compounds, and the bond strength of Nb–O becomes stronger with a structure containing strontium. Furthermore, the splitting of A_{1g} mode disappeared gradually in Sr-rich compounds at $x \geq 0.6$. The wave number of A_{1g} mode for Sr-rich compounds was observed to be almost constant at 802–805 cm^{-1}.

The F_{2g} mode showed a narrow splitting at 306 and 318 cm^{-1} for $Ba_5Nb_4O_{15}$ compound. This narrow doublet was due to the empty octahedra and it was caused by a small local departure from the $P\bar{3}m1$ space group.[5] The behavior of F_{2g} active modes indicated that its centrosymmetry was locally lost in $Ba_5Nb_4O_{15}$ compounds. This narrow doublet gradually disappeared with an

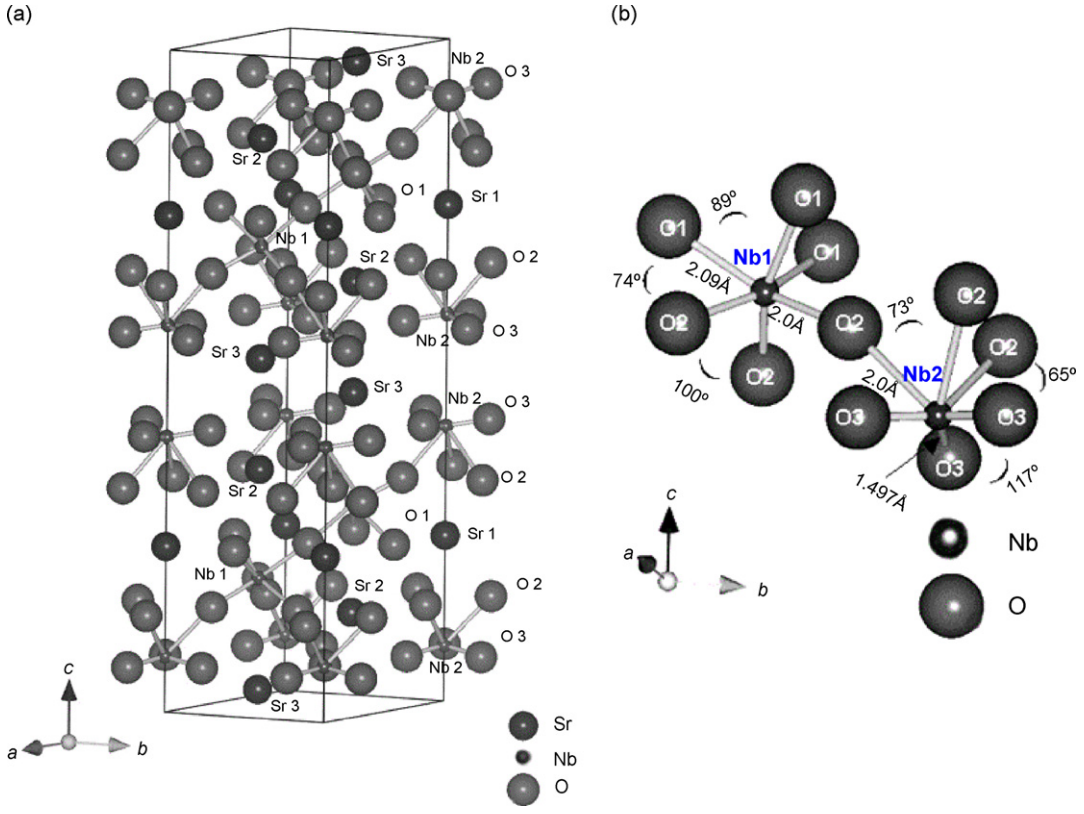

Fig. 5. (a) Crystal structure of $Sr_5Nb_4O_{15}$ compound with refined XRD data. (b) Description of bond lengths and angles in NbO_6 octahedra for $Sr_5Nb_4O_{15}$ compound.

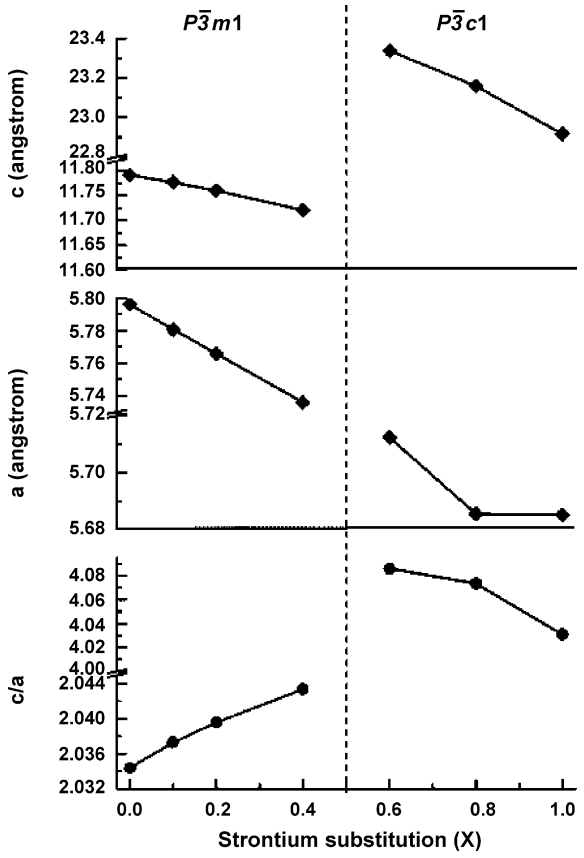

Fig. 6. Variation of lattice parameter a, c and (c/a) ratio as a function of Sr^{2+} substitution (x).

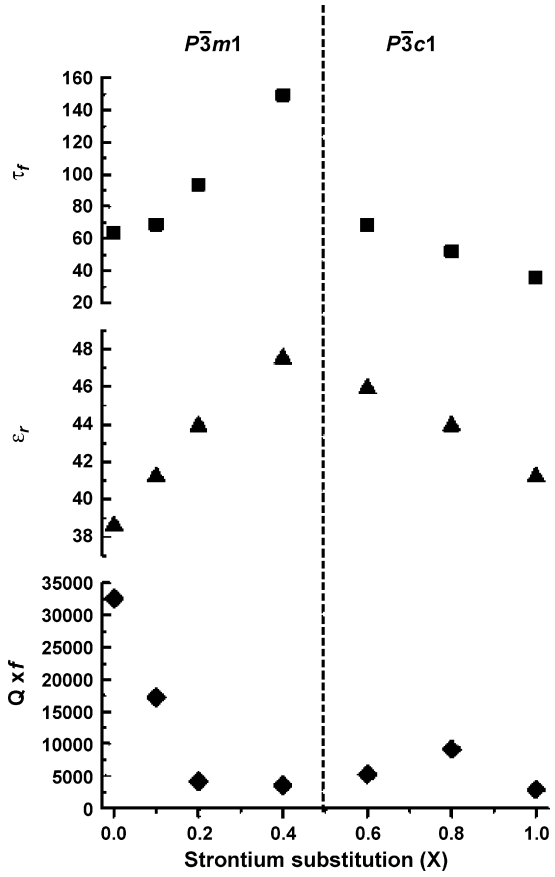

Fig. 7. Variation of ε_r and τ_f as a function of Sr^{2+} substitution (x).

increase of strontium content in Ba-rich of composition, $x \leq 0.4$. However, the splitting of F_{2g} mode was present again in Sr-rich compounds and shifted to higher wave-number of region with the increase of strontium content. The splitting of F_{2g} mode was located at 317 and 331 cm^{-1} for $Sr_5Nb_4O_{15}$ compound. The transition of symmetry from $P\bar{3}m1$ to $P\bar{3}c1$ space group also could be probed from above variation of F_{2g} mode.

4. Discussion

The Nb^{5+} was too small to form regular NbO_6 octahedra and therefore resulted in the distortion. The local charge imbalance of empty octahedra in the cation-deficient perovskites compound also caused the distortion of oxygen octahedra. The bond distance of Nb(2)–O(3) ions became shortened and was compensated by the lengthening of Nb(2)–O(2) bonding distance to maintain the structure of NbO_6 octahedra. The presence of different Nb–O bond lengths may be the reason for large splitting of symmetric stretching mode of oxygen octahedra. The analysis of A_{1g} and F_{2g} modes in Raman spectra indicates a structure transition between Ba-rich and Sr-rich compounds. This result confirms the study of Rietveld analysis for X-ray diffraction patterns where the symmetry of crystal structure changed from $P\bar{3}m1$ to $P\bar{3}c1$ space group in Sr-rich compounds.

Dielectric constant is determined by the ionic and electronic polarization in the microwave region, and ionic contribution is the most important for the higher dielectric constant of compounds. The experimental permittivity data was used to compare the dielectric polarizability with that predicted by the ion additivity rule reported by Shannon.[21] The experimental dielectric constant was corrected for the porosity of the ceramics to calculate the dielectric polarizability and compare the values to those obtained from the sum of Shannon's polarizabilities:

$$\varepsilon_{r,corr} = \varepsilon_{r,exp.} \times \frac{2+P}{2-2P}$$

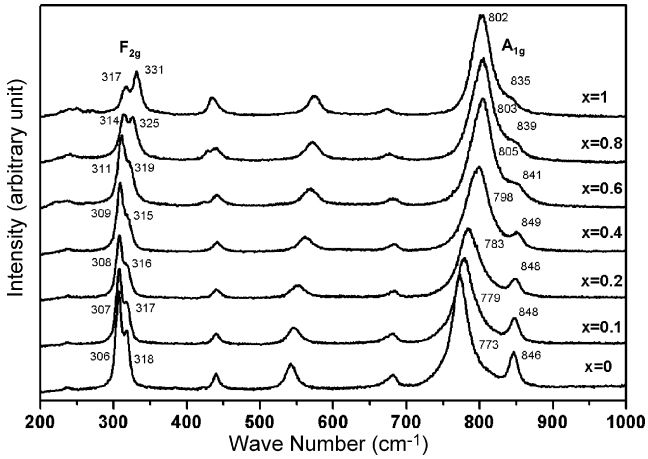

Fig. 8. Raman spectra of the $(Ba_{1-x}Sr_x)_5Nb_4O_{15}$ compounds.

Table 2
Calculated and predicated dielectric polarizability of $(Ba_{1-x}Sr_x)_5Nb_4O_{15}$ compounds

Compound	Space group	$\varepsilon_{r,exp.}$	Density (% theor.)	$\varepsilon_{r,corr}$	V_m (Å^3)	$\alpha_{exp.}$ (Å^3)	$\alpha_{Shannon.}$(Å^3)
$Ba_5Nb_4O_{15}$	$P\bar{3}m1$	38.6	92.1	43.63	342.82	76.46	78.03
$Ba_{4.5}Sr_{0.5}Nb_4O_{15}$	$P\bar{3}m1$	41.2	93.2	45.85	340.64	76.22	76.95
$Ba_4Sr_1Nb_4O_{15}$	$P\bar{3}m1$	43.9	93.5	48.48	338.33	75.97	75.87
$Ba_3Sr_2Nb_4O_{15}$	$P\bar{3}m1$	47.5	93.0	52.86	333.82	75.34	73.71
$Ba_2Sr_3Nb_4O_{15}$	$P\bar{3}c1$	45.9	92.5	51.48	329.77	74.31	71.55
$Ba_1Sr_4Nb_4O_{15}$	$P\bar{3}c1$	43.9	94.5	47.73	324.16	72.72	69.39
$Sr_5Nb_4O_{15}$	$P\bar{3}c1$	41.2	96.1	43.78	320.72	71.55	67.23

where $\varepsilon_{r,corr}$ is the corrected permittivity, $\varepsilon_{r,exp.}$ the measured permittivity and P is the porosity.

This calculation of dielectric polarizability was conducted using the Clausius–Mossotti equation:

$$\alpha = \frac{1}{b}\left[\frac{(V_m)(\varepsilon_{r,corr}-1)}{\varepsilon_{r,corr}+2}\right]$$

where V_m is the molar cell volume ($=V_{unit\ cell}/Z$) and $b=4\pi/3$.

The Ba-rich compounds have one formula unit per Bravais cell ($Z=1$) in the hexagonal system with space group of $P\bar{3}m1$. The Sr-rich compounds with $P\bar{3}c1$ space group showed that $Z=2$. If large deviations would occur between $\varepsilon_{r,calc}$ and $\varepsilon_{r,exp.}$, it would generally reflect a situation similar to inaccurate dielectric constant, ionic or electronic conductivity, the presence of "rattling" or "compressed" cation having large or small polarizabilities, or the presence of dipolar impurities. Vineis et al.[22] showed that the dielectric polarizability of $Ba_5Nb_4O_{15}$ calculated from experiment is 76.35 Å^3 which is in agreement with the sum of the ion polarizabilities. Table 2 shows that the polarizability of $Ba_5Nb_4O_{15}$ for our experiment was 76.46 Å^3, which coincided with the previous investigation.

Table 2 indicates that dielectric polarizability of these compounds calculated from experiment was in reasonable agreement with the sum of the ion polarizabilities proposed by Shannon. The above special situations should not happen in the $(Ba_{1-x}Sr_x)_5Nb_4O_{15}$ system. It was evident that the polarizabilities of $\alpha_{exp.}$ and $\alpha_{Shannon}$ were both decreased linearly with an increase of strontium content. This was due to the smaller ionic polarizability for strontium than that of barium ion.

The Ba-rich compounds are characterized by a strong anharmonic lattice where the symmetric stretching vibration, A_{1g} mode, splits into two narrow Raman-active modes. This indicates that the lattice had a small local departure from the reported centrosymmetric $D^3_{3d}-P\bar{3}m1$ space group, and changed into a lower symmetry structure. The splitting A_{1g} modes in anharmonic lattice gradually shifted to high wave-number region in Ba-rich composition from Raman analysis. However, the ε_r and τ_f linearly increase in Ba-rich compounds and decrease in Sr-rich compounds with an increase of strontium content. This showed a distinct correlation between the magnitude of ε_r and the (c/a) ratio of lattice parameter in Ba-rich compounds. The increase of (c/a) ratio showed the stretch of crystal structure along the c-axis with strontium substitution. Based on the observation, lattice anharmonicity increased with the increase of lattice parameter (c/a) ratio and upward shifting frequency of symmetric stretching modes, A_{1g}. This resulted in an increase of ε_r in Ba-rich compounds even though the ionic polarizability decreased gradually with strontium substitution. However, the structural transition from $P\bar{3}m1$ to $P\bar{3}c1$ caused the decrease of ε_r. The (c/a) ratio and ionic polarizability decreased and this resulted in the decrease of ε_r with an increase of strontium content in Sr-rich compounds.

The τ_f is related to the temperature coefficient of relative permittivity (τ_ε):

$$\tau_f = -\frac{1}{2}\tau_\varepsilon - \alpha$$

where α is the thermal expansion coefficient. The τ_f was directly influenced by τ_ε, since the magnitude of α was generally constant and insignificant compared to that of $\tau_{\varepsilon.}$:

$$\tau_\varepsilon = \frac{(\varepsilon-1)(\varepsilon+2)}{3\varepsilon}(A+B+C)$$

The (A) term represents a direct dependence of the polarizability on temperature. Colla et al.[23] suggested that the (A) term generally determines the sign and magnitude of τ_ε. This depends on the structure of the compounds rather than their compositions. Fig. 7 show that the τ_f abruptly decrease at $x=0.6$. This indicates that the transition of symmetry from $P\bar{3}m1$ to $P\bar{3}c1$ space group influenced the τ_ε and resulted in the abrupt decrease of τ_f in Sr-rich compounds. Reaney et al.[24] showed that the onset of tilting transition was the major factor that influenced the behavior of τ_ε. The tilting of oxygen octahedra has been investigated in conjunction with τ_ε. The decrease in tolerance factor by cation substitution induced the tilting of oxygen octahedra and caused the transition of τ_f as a function of composition. The c-parameter is doubled due to an anti-tilting of octahedra around the c-axis in Sr-rich compounds with $P\bar{3}c1$ symmetry. The transition of symmetry that involved with the tilting of NbO_6 octahedra resulted in the decrease of τ_f and this phenomenon was coincided with the investigation of Reaney.

5. Conclusion

A considerable distortion of NbO_6 octahedra was observed, which indicates that lattice anharmonicity exists in the structure of $(Ba_{1-x}Sr_x)_5Nb_4O_{15}$ system. The symmetry of crystal structure changed from $P\bar{3}m1$ to $P\bar{3}c1$ with strontium substitution from the Rietveld analysis of X-ray diffraction patterns.

The linear increase of ε_r and τ_f was observed by accompanying the increase of lattice parameter (c/a) ratio and the

upward frequency shifting for the symmetric stretching vibration of NbO_6 octahedra in Ba-rich compounds. However, the Sr-rich compounds with $P\bar{3}c1$ symmetry show a decrease in (c/a) ratio and ionic polarizability, which results in the gradual decrease of ε_r with strontium substitution. The transition of symmetry from $P\bar{3}m1$ to $P\bar{3}c1$ space group resulted in the tilting of oxygen octahedra and caused the abrupt decrease of τ_f in Sr-rich compound.

Acknowledgement

Supported by the National Science Council of Taiwan under Contract No. NSC 94-2216-E-006-045.

References

1. Jawahar, I. N., Mohanan, P. and Sebastian, M. T., $A_5B_4O_{15}$ (A = Ba, Sr, Mg, Ca, Zn; B = Nb, Ta) microwave dielectric ceramics. *Mater. Lett.*, 2003, **57**, 4043–4048.
2. Kamba, S., Petzelt, J., Haubrich, D., Vanek, P., Kuzel, P., Jawahar, I. N., Sebastian, M. T. and Mohanan, P., High frequency dielectric properties of $A_5B_4O_{15}$ microwave ceramics. *J. Appl. Phys.*, 2001, **89**(7), 3900–3906.
3. Jawahar, I. N., Sebastian, M. T. and Mohanan, P., Microwave dielectric properties of $Ba_{5-x}Sr_xTa_4O_{15}$ $Ba_5Nb_xTa_{4-x}O_{15}$ and $Sr_5Nb_xTa_{4-x}O_{15}$ ceramics. *Mater. Sci. Eng.*, 2004, **B106**, 207–212.
4. Galasso, F. and Katz, L., Preparation and structure of $Ba_5Ta_4O_{15}$ and related compounds. *Acta Cryst.*, 1961, **14**, 647–650.
5. Massa, N. E., Pagola, S. and Carbonio, P., Far-infrared reflectivity and Raman spectra of $Ba_5Nb_4O_{15}$. *Phys. Rev.*, 1996, **B53**(13), 8148–8150.
6. Shannon, J. and Katz, L., A refinement of the structure of barium tantalum oxide, $Ba_5Ta_4O_{15}$. *Acta Cryst.*, 1970, **B26**, 102–105.
7. Pagola, S., Carbonio, R. E., Fernandez-Diaz, M. T. and Alonso, J. A., Crystal structure refinement of $Mg_5Nb_4O_{15}$ and $Mg_5Ta_4O_{15}$ by Rietveld analysis of neutron powder diffraction data. *J. Solid State Chem.*, 1998, **137**, 359–364.
8. Kim, D. W., Youn, H. J., Hong, K. S. and Kim, C. K., Microwave dielectric properties of $(1-x)Ba_5Nb_4O_{15}$–$xBaNb_2O_6$ mixtures. *Jpn. J. Appl. Phys.*, 2002, **41**, 3812–3816.
9. Kim, D. W., Kim, J. R., Yoon, S. H., Hong, K. S. and Kim, C. K., Microwave dielectric properties of low-fired $Ba_5Nb_4O_{15}$. *J. Am. Ceram. Soc.*, 2002, **85**(11), 2759–2762.
10. Kim, D. W., Hong, K. S., Yoon, C. S. and Kim, C. K., Low-temperature sintering and microwave dielectric properties of $Ba_5Nb_4O_{15}$–$BaNb_2O_6$ mixture for LTCC application. *J. Eur. Ceram. Soc.*, 2003, **23**, 2597–2601.
11. Kim, D. W., Kwon, D. K., Hong, K. S. and Kim, D. J., Atmospheric dependence on dielectric loss of 1/6 $Ba_5Nb_4O_{15}$–5/6$BaNb_2O_6$ ceramics. *J. Am. Ceram. Soc.*, 2003, **86**(5), 795–799.
12. Sreemoolanadhan, H., Sebastian, M. T. and Mohanan, P., High permittivity and low loss ceramics in the BaO–SrO–Nb_2O_5 system. *Mater. Res. Bull.*, 1995, **30**(6), 653–658.
13. Ratheesh, R., Sreemoolanadhan, H. and Sebastian, M. T., Vibrational analysis of $Ba_{5-x}Sr_xNb_4O_{15}$ microwave dielectric ceramic resonators. *J. Solid State Chem.*, 1997, **131**, 2–8.
14. Blasse, G. and Van Den Heuvel, G. P. M., Vibration spectra and structural considerations of compounds $NaLnTiO_4$. *J. Solid State Chem.*, 1974, **10**, 206–210.
15. Lee, C. J., Pezotti, G., Kang, S. H., Kim, D. J. and Hong, K. S., Quantitative analysis of lattice distortion in $Ba(Zn_{1/3}Ta_{2/3})O_3$ microwave dielectric ceramics with added B_2O_3 using Raman spectroscopy. *J. Eur. Ceram. Soc.*, 2006, **26**, 1385–1391.
16. Nagai, T., Sugiyama, M., Sando, M. and Niihara, K., Anomaly in the infrared active phonon modes and its relationship to the dielectric constant of $(Ba_{1-x}Sr_x)(Mg_{1/3}Ta_{2/3})O_3$ compound. *Jpn. J. Appl. Phys.*, 1996, **35**, 5163–5167.
17. Larson, A. C. and Von Dreele, R. B., *General Structure Analysis System (GSAS)*. Los Alamos National Laboratory, Los Alamos, 1988.
18. Weiden, M., Grauel, A., Norwig, J., Horn, S. and Steglich, F., Crystalline structure of the strontium niobates $Sr_4Nb_2O_9$ and $Sr_5Nb_4O_{15}$. *J. Alloys Compd.*, 1995, **218**, 13–16.
19. Whiston, C. D. and Smith, A. J., Double oxides containing niobium or tantalum. II. System involving strontium or barium. *Acta Crystallogr.*, 1967, **23**, 82.
20. Teneze, N., Mercurio, D., Trolliard, G. and Champarnaud-Mesjard, J. C., Reinvestigation of the crystal structure of pentastrontium tetraniobate $Sr_5Nb_4O_{15}$. *Z. Kristallogr. NICS*, 2000, **215**, 11–12.
21. Shannon, R. D., Dielectric polarizabilities of ions in oxides and fluorides. *J. Appl. Phys.*, 1993, **73**, 348–366.
22. Vineis, C., Davies, P. K., Negas, T. and Bell, S., Microwave dielectric properties of hexagonal perovskites. *Mater. Res. Bull.*, 1996, **31**(5), 431–437.
23. Colla, E. L., Reaney, I. M. and Setter, N., Effect of structural changes in complex perovskites on the temperature coefficient of the relative permittivity. *J. Appl. Phys.*, 1993, **74**(5), 3414–3425.
24. Reaney, I. M., Colla, E. L. and Setter, N., Dielectric and structural characteristics of Ba- and Sr-based complex perovskites as a function of tolerance factor. *Jpn. J. Appl. Phys.*, 1994, **33**, 3984–3990.